Title: A perspective on causal dynamical triangulations in 3+1 vignettes

Date: Dec 04, 2014 02:30 PM

URL: http://pirsa.org/14120007

Abstract: <p>I offer a personal perspective on the causal dynamical triangulations approach to the construction of quantum theories of gravity. After briefly introducing the approach's formalism and results, I illuminate this perspective with 3+1 vignettes of recent and ongoing research. Specifically, I review attempts to locate an ultraviolet fixed point through renormalization group analyses; I report measurements of the homogeneity of the approach's quantum geometries; I discuss efforts to determine the large scale effective action in the case of 2+1 dimensions; and I suggest a speculative possibility for reviving the Euclidean dynamical triangulations approach.</p>

Quantum gravity as quantum field theory

Introduction

Quantum gravity as quantum field theory

Will the quantum theory of gravity prove to be yet another triumph of the paradigm of the quantum theory of fields?

Facts to keep in mind

- Einstein gravity is perturbatively nonrenormalizable. ['t Hooft and Veltman 1974], [Goroff and Sagnotti 1986]
- Perturbative quantum Einstein gravity is a consistent effective field theory. [Donoghue 2012]
- The Planck length ℓ_{P} generically sets the scale of perturbative quantum gravitational effects.

Potential responses

- Perturbatively renormalizable modified theories of gravity [Stelle 1977], [Hořava 2009], *et cetera*
- Asymptotic safety [Weinberg 1979], [Reuter 1996]
- Non-field-theoretic quantum gravity (loop quantum gravity, causal sets, *et cetera*)

Nonperturbative field-theoretic approaches

- Exact renormalization group

Causal dynamical triangulations

A prescription for making sense of the gravitational path integral patterned on standard lattice quantum field-theoretic techniques

1. Restrict the path integration to 'causal' spacetimes.
   - A causal spacetime admits a global foliation by spacelike hypersurfaces all of the same topology.
2. Regularize causal spacetimes by causal triangulations.
   - A causal triangulation $\mathcal{T}_c$ is a piecewise-Minkowski simplicial manifold admitting a global foliation by spacelike hypersurfaces all of the same topology.

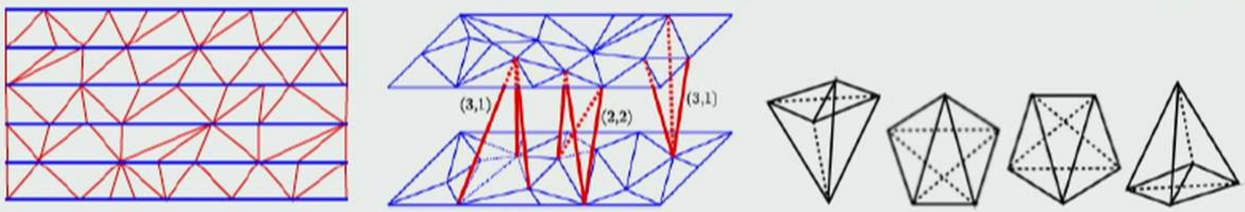

$$\ell_{\mathrm{SL}}^2 = a^2$$
$$\ell_{\mathrm{TL}}^2 = -\alpha a^2$$

[Jordan and Loll 2013]

3. Replace the formal path integral $\mathscr{A}_\Sigma[h]$ with the concrete path sum $\mathcal{A}_\Sigma[\Gamma]$.

$$\mathscr{A}_\Sigma[h] = \int_{\substack{\mathscr{M}\cong\Sigma\times[0,1] \\ \mathbf{g}|_{\partial\mathscr{M}}=h}} \mathrm{d}\mu(\mathbf{g})\, e^{iS_{\mathrm{cl}}[\mathbf{g}]/\hbar} \longrightarrow \mathcal{A}_\Sigma[\Gamma] = \sum_{\substack{\mathcal{T}_c\cong\Sigma\times[0,1] \\ \mathcal{T}_c|_{\partial\mathcal{T}_c}=\Gamma}} \frac{1}{C(\mathcal{T}_c)}\, e^{i\mathcal{S}_{\mathrm{cl}}[\mathcal{T}_c]/\hbar}$$

4. Compute the path sum $\mathcal{A}_\Sigma[\Gamma]$.
5. Take the continuum limit (if it exists).

Causal dynamical triangulations in practice

A prescription for making sense of the gravitational path integral patterned on standard lattice quantum field-theoretic techniques

1. Restrict the path integration to 'causal' spacetimes.
2. Regularize causal spacetimes by causal triangulations.
3. Replace the formal path integral $\mathscr{A}_\Sigma[h]$ with the concrete path sum $\mathcal{A}_\Sigma[\Gamma]$.

$$\mathscr{A}_\Sigma[h] = \int_{\substack{\mathscr{M}\cong\Sigma\times[0,1] \\ \mathbf{g}|_{\partial\mathscr{M}}=h}} \mathrm{d}\mu(\mathbf{g})\, e^{iS_{\mathrm{cl}}[\mathbf{g}]/\hbar} \longrightarrow \mathcal{A}_\Sigma[\Gamma] = \sum_{\substack{\mathcal{T}_c\cong\Sigma\times[0,1] \\ \mathcal{T}_c|_{\partial\mathcal{T}_c}=\Gamma}} \frac{1}{C(\mathcal{T}_c)}\, e^{i\mathcal{S}_{\mathrm{cl}}[\mathcal{T}_c]/\hbar}$$

4. Wick rotate to the Euclidean domain.

$$\mathcal{A}_\Sigma[\Gamma] = \sum_{\mathcal{T}_c|_{\partial\mathcal{T}_c}=\Gamma} \frac{1}{C(\mathcal{T}_c)}\, e^{i\mathcal{S}_{\mathrm{cl}}[\mathcal{T}_c]/\hbar} \longrightarrow \mathcal{Z}_\Sigma[\Gamma] = \sum_{\mathcal{T}_c|_{\partial\mathcal{T}_c}=\Gamma} \frac{1}{C(\mathcal{T}_c)}\, e^{-\mathcal{S}_{\mathrm{cl}}^{(\mathrm{E})}[\mathcal{T}_c]/\hbar}$$

5. Run Monte Carlo simulations of representative causal triangulations.
6. Wick rotate back to the Lorentzian domain.
7. Take the continuum limit (if it exists).

First key result: phase structure

Quantization of $(3+1)$-dimensional Einstein gravity
with $\Lambda > 0$ and $\mathcal{T}_c \cong S^3 \times S^1$

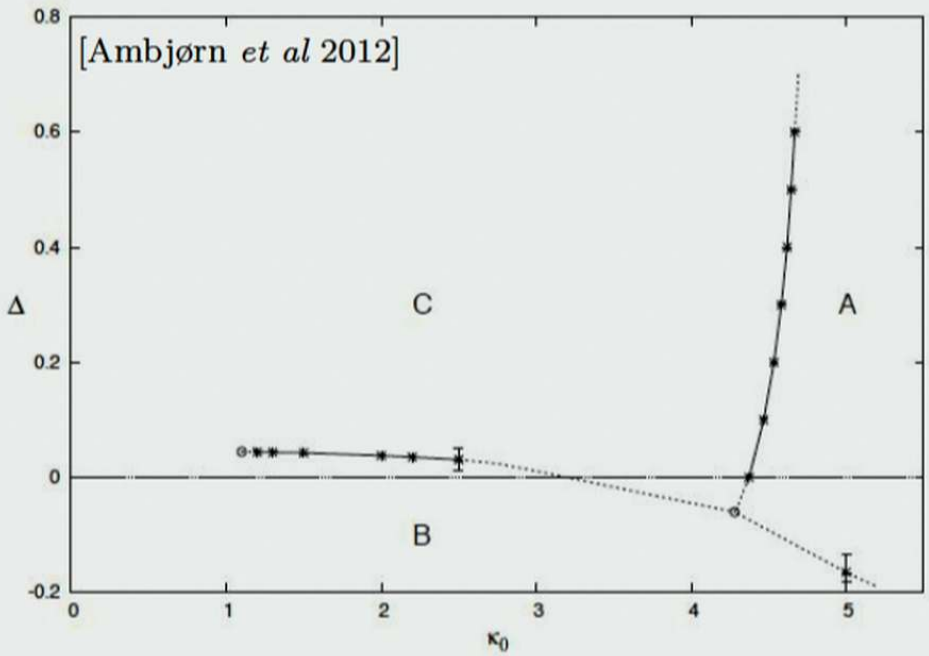

AC phase transition is first order

BC phase transition is second order

Phase A

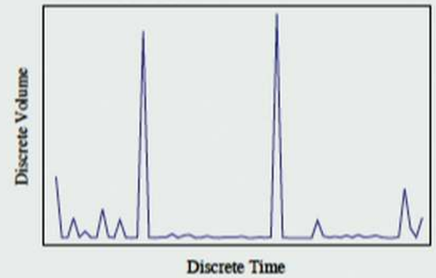

Phase B

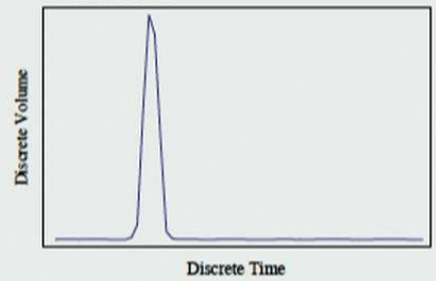

Phase C

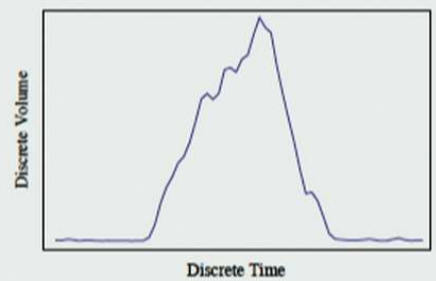

Second key result: classical limit

Large scale effective action for the discrete spatial volume $N_3(\tau)$

$$S_{\text{eff}}^{(\text{E})}[N_3] = c_1 \sum_\tau \left\{ \frac{[N_3(\tau+1) - N_3(\tau-1)]^2}{4N_3(\tau)} + c_2 N_3^{1/3}(\tau) + c_3 N_3(\tau) \right\}$$

Corresponding effective action for the continuous spatial volume $V_3(t)$

$$S_{\text{eff}}^{(\text{E})}[V_3] = \frac{1}{24\pi G_{\text{ren}}} \int \mathrm{d}t \sqrt{g_{tt}} \left\{ \frac{[\mathrm{d}V_3(t)/\mathrm{d}t]^2}{g_{tt} V_3(t)} + 9(2\pi^2)^{2/3} V_3^{1/3}(t) - \Lambda_{\text{ren}} V_3(t) \right\}$$

Extremum: Euclidean de Sitter space

$$V_3^{(\text{EdS})}(t) = 2\pi^2 \ell_{\text{dS}}^3 \cos^3\left(\frac{\sqrt{g_{tt}}\,t}{\ell_{\text{dS}}}\right)$$

Finite size scaled

$$\langle N_3^{(\text{EdS})}(\tau)\rangle \propto \frac{N_4}{s_0 N_4^{1/4}} \cos^3\left(\frac{\tau}{s_0 N_4^{1/4}}\right)$$

1-point function $\langle N_3(\tau)\rangle$

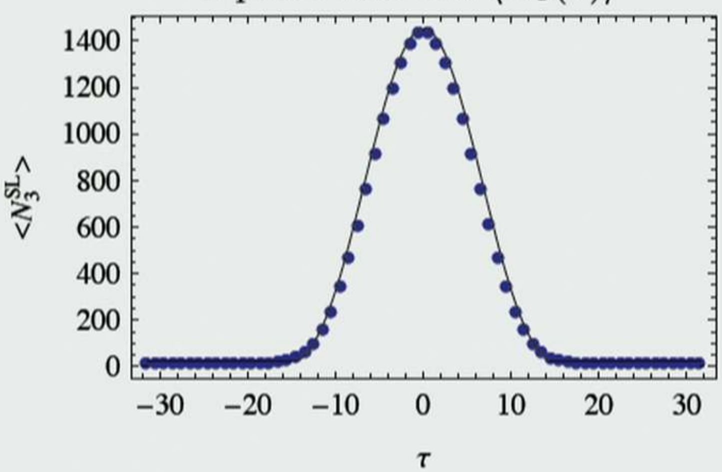

Second key result: semiclassical limit

Connected 2-point function $\langle n_3(\tau) n_3(\tau')\rangle$ of fluctuations $n_3(\tau) = N_3(\tau) - \langle N_3(\tau)\rangle$

$$\langle n_3(\tau) n_3(\tau')\rangle = \gamma^2 N_4 F\left(\frac{\tau}{s_0 N_4^{1/4}}, \frac{\tau'}{s_0 N_4^{1/4}}\right) \quad \text{with } \gamma^2 \sim G_{\text{ren}}\Lambda_{\text{ren}} \sim \frac{\ell_{\text{P}}^2}{\ell_{\text{dS}}^2}$$

Connected 2-point function $\langle v_3(t) v_3(t')\rangle$ of fluctuations $v_3(\tau) = V_3(t) - V_3^{(\text{EdS})}(t)$

$$\langle v_3(t) v_3(t')\rangle = \left.\frac{\delta^2 S_{\text{eff}}^{(\text{E})}[V_3]}{\delta v_3(t)\delta v_3(t')}\right|_{v_3(t)=0} \quad \text{at } O(v_3^2(t))$$

Eigenvectors

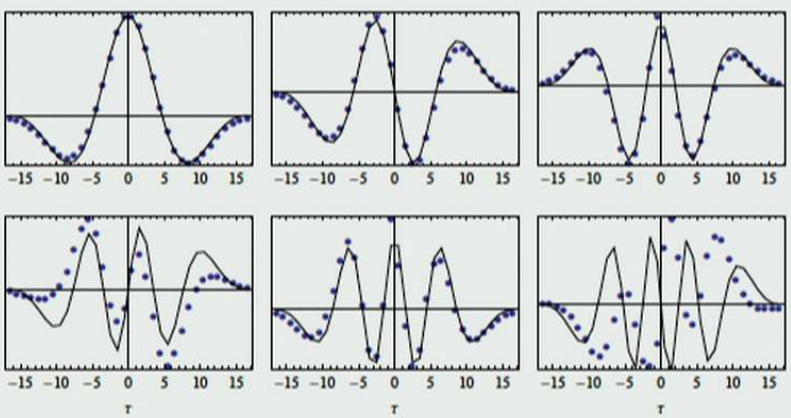

Eigenvalues

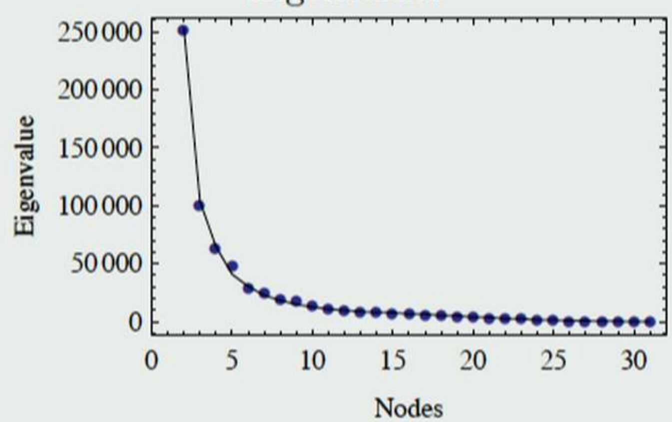

Third key result: quantum mechanical effect

Diffusion on a Wick rotated causal triangulation $\mathcal{T}_c$

$$K(s, s', \sigma + 1) = (1 - \rho)K(s, s', \sigma) + \frac{\rho}{N(\mathcal{N}_s(1))} \sum_{s'' \in \mathcal{N}_s(1)} K(s'', s', \sigma)$$

Return probability $P(\sigma)$

$$P(\sigma) = \frac{1}{N_4} \sum_{s \in \mathcal{T}_c} K(s, s, \sigma)$$

Spectral dimension

$$D_s(\sigma) = -2\frac{\mathrm{d} \ln P(\sigma)}{\mathrm{d} \ln \sigma}$$

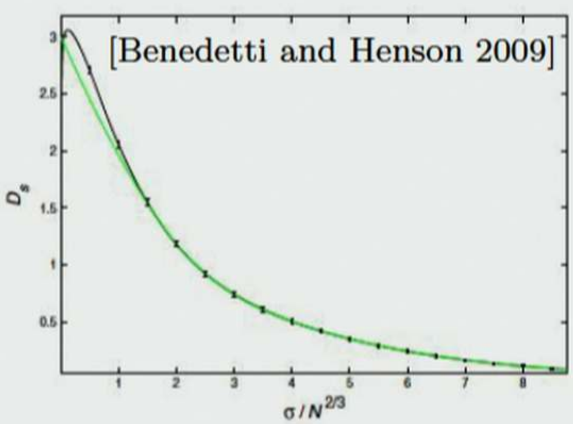

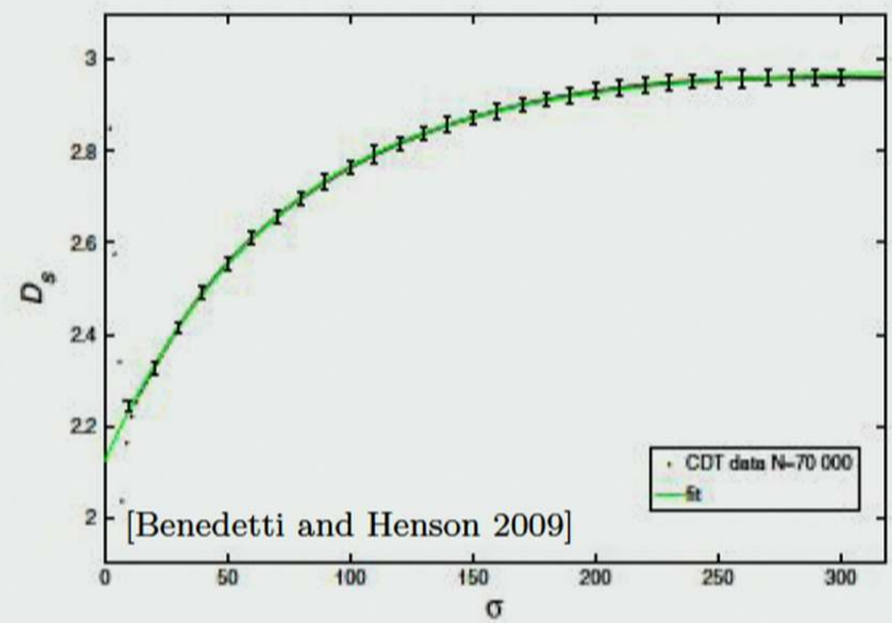

Extrapolated to $D_s(0) \approx 2$

Third key result: quantum mechanical effect

Diffusion on a Wick rotated causal triangulation $\mathcal{T}_c$

$$K(s,s',\sigma+1) = (1-\rho)K(s,s',\sigma) + \frac{\rho}{N(\mathcal{N}_s(1))} \sum_{s'' \in \mathcal{N}_s(1)} K(s'',s',\sigma)$$

Return probability $P(\sigma)$

$$P(\sigma) = \frac{1}{N_4} \sum_{s \in \mathcal{T}_c} K(s,s,\sigma)$$

Spectral dimension

$$D_s(\sigma) = -2 \frac{\mathrm{d} \ln P(\sigma)}{\mathrm{d} \ln \sigma}$$

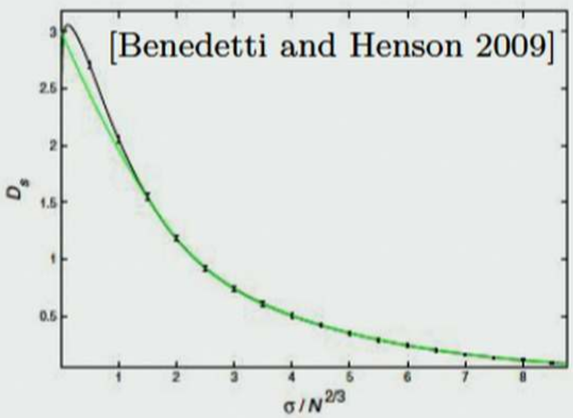

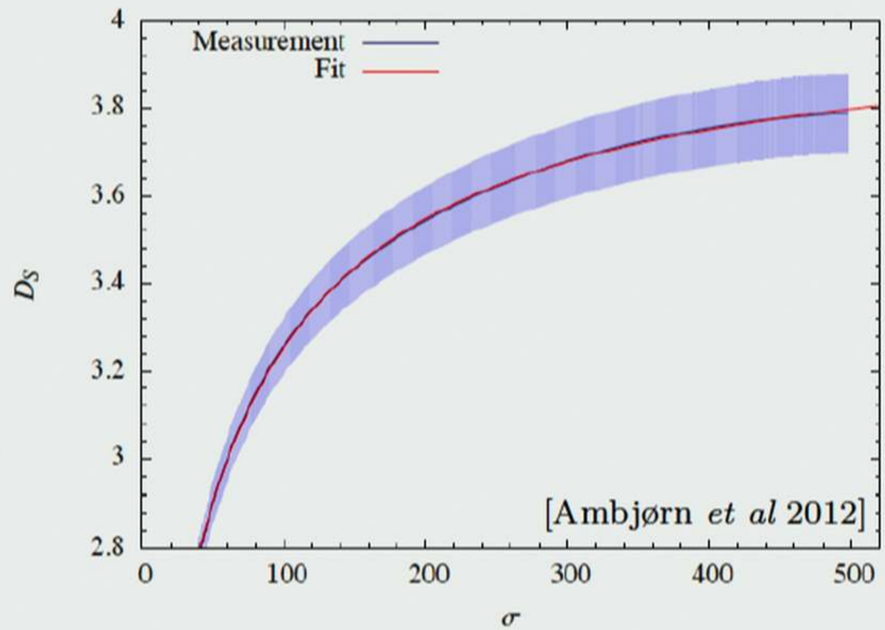

Extrapolated to $D_s(0) \approx 2$

but see [Coumbe and Jurkiewicz 2014]

First vignette: Renormalization group flows

Renormalization group flows from lattice data

Delineating renormalization group trajectories

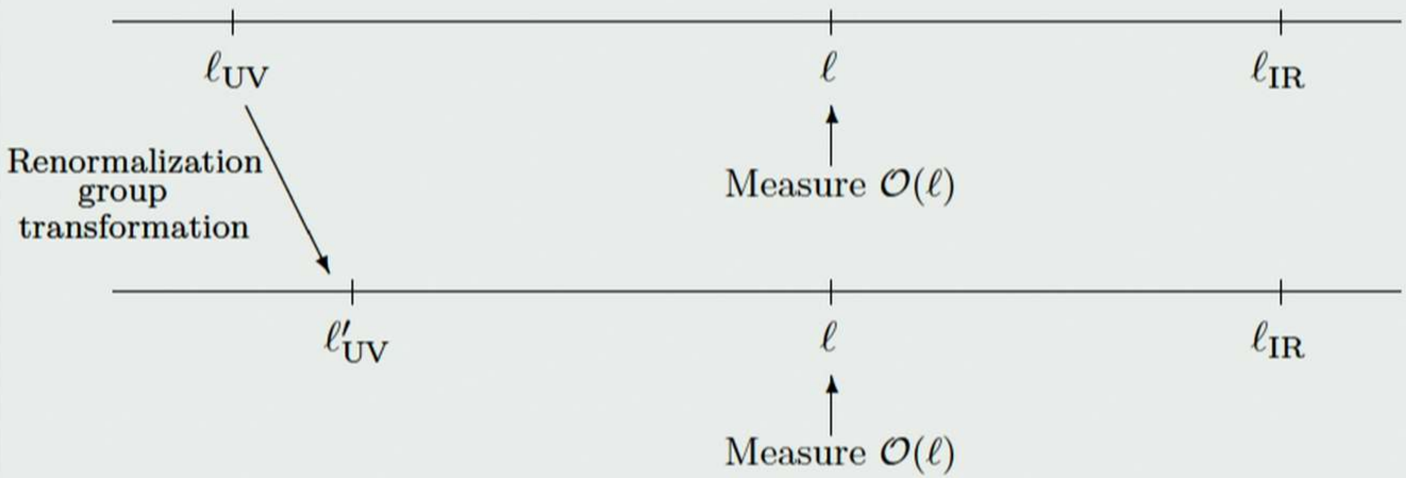

Agreement of measurements of the physical observable $\mathcal{O}(\ell)$ before and after the renormalization group transformation

Implementing renormalization group transformations

Standard technique: Repeatedly coarse grain each of the causal triangulations in an initial ensemble.

Alternative technique: Directly generate ensembles of causal triangulations characterized by different ranges of scales by varying the control parameters T, N_4, κ_0, and Δ.

Status report on renormalization group analyses

- My renormalization group scheme [JHC 2014a, 2014b]
  - Model: Minisuperspace approximation of the Euclidean Einstein-Hilbert action with Euclidean de Sitter space (plus quadratic fluctuations) as the ground state
  - Observables: V_4, $G_{\text{ren}}\Lambda_{\text{ren}}$, and $D_s(\sigma)$, not $\langle N_3(\tau)\rangle$, $\langle n_3(\tau)n_3(\tau')\rangle$, or s_0
  - Status: Insufficiently many physical observables to delineate renormalization group trajectories

- Ambjørn *et al*'s renormalization group scheme [Ambjørn *et al* 2014]
  - Model: Minisuperspace approximation of a Euclidean Hořava-Lifshitz action with deformed Euclidean de Sitter space (plus quadratic fluctuations) as the ground state
  - Observables: V_4, $G_{\text{ren}}\Lambda_{\text{ren}}$, and $D_s(\sigma)$, also $\langle N_3(\tau)\rangle$, $\langle n_3(\tau)n_3(\tau')\rangle$, and s_0
  - Assumption: Lattice spacing is constant for all values of κ_0 and Δ in phase C
  - Status: Tentative evidence for an ultraviolet fixed point along the BC phase transition

Second vignette: Homogeneity measures

Scale-dependent homogeneity measures

- Motivation
  - Define novel physical observables
  - Derive spectrum of primordial cosmological perturbations from causal dynamical triangulations

- Inspiration
  - Techniques to assess the homogeneity of our own universe
    - Galaxy redshift surveys [Scrimgeour *et al* 2012]

- Application
  - Measure homogeneity of the quantum spacetime geometry
  - Measure temporal evolution (in the distinguished foliation) of the homogeneity of the quantum spatial geometry

[JHC 2014c]

Volumetric homogeneity measure

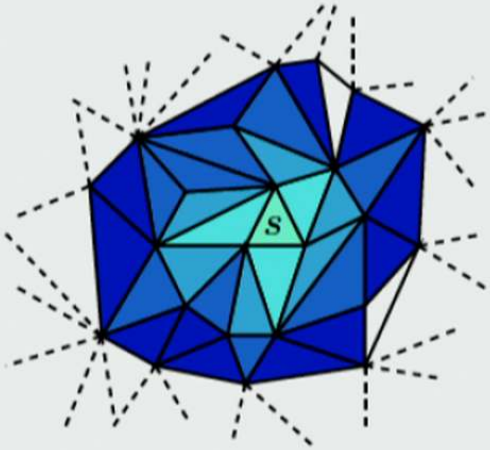

r	$N(\mathscr{N}_s(r))$
0	1
1	3
2	6
3	9
4	12
⋮	⋮

[JHC 2014c]

- Number of simplices within graph distance r

$$\mathfrak{N}_s(r) = \frac{1}{N_D} \sum_{r'=0}^{r} N(\mathscr{N}_s(r'))$$

  - Mean

$$\mathrm{E}[\mathfrak{N}(r)] = \frac{1}{N_D} \sum_{s \in \mathcal{T}} \mathfrak{N}_s(r)$$

  - Variance

$$\mathrm{Var}[\mathfrak{N}(r)] = \frac{1}{N_D - 1} \sum_{s \in \mathcal{T}} \{\mathfrak{N}_s(r) - \mathrm{E}[\mathfrak{N}(r)]\}^2$$

- Hausdorff dimension

$$d_H(r) = \frac{\mathrm{d} \ln \mathrm{E}[\mathfrak{N}(r)]}{\mathrm{d} \ln r}$$

- Homogeneity measure

$$\begin{aligned} \mathrm{H}_{\mathrm{vol}}(r) &= \langle \mathrm{Var}[\mathfrak{N}(r)] \rangle \\ &= \frac{1}{Z_\Sigma} \sum_{\mathcal{T}} \mu(\mathcal{T})\, e^{-\mathcal{S}^{(\mathrm{E})}[\mathcal{T}]}\, \mathrm{Var}[\mathfrak{N}_{\mathcal{T}}(r)] \end{aligned}$$

Finite size scaling of spacetime volumetric homogeneity

Ensembles of causal triangulations in phase C ($\mathcal{T}_c \cong S^2 \times S^1$, $k_0 = 1$)

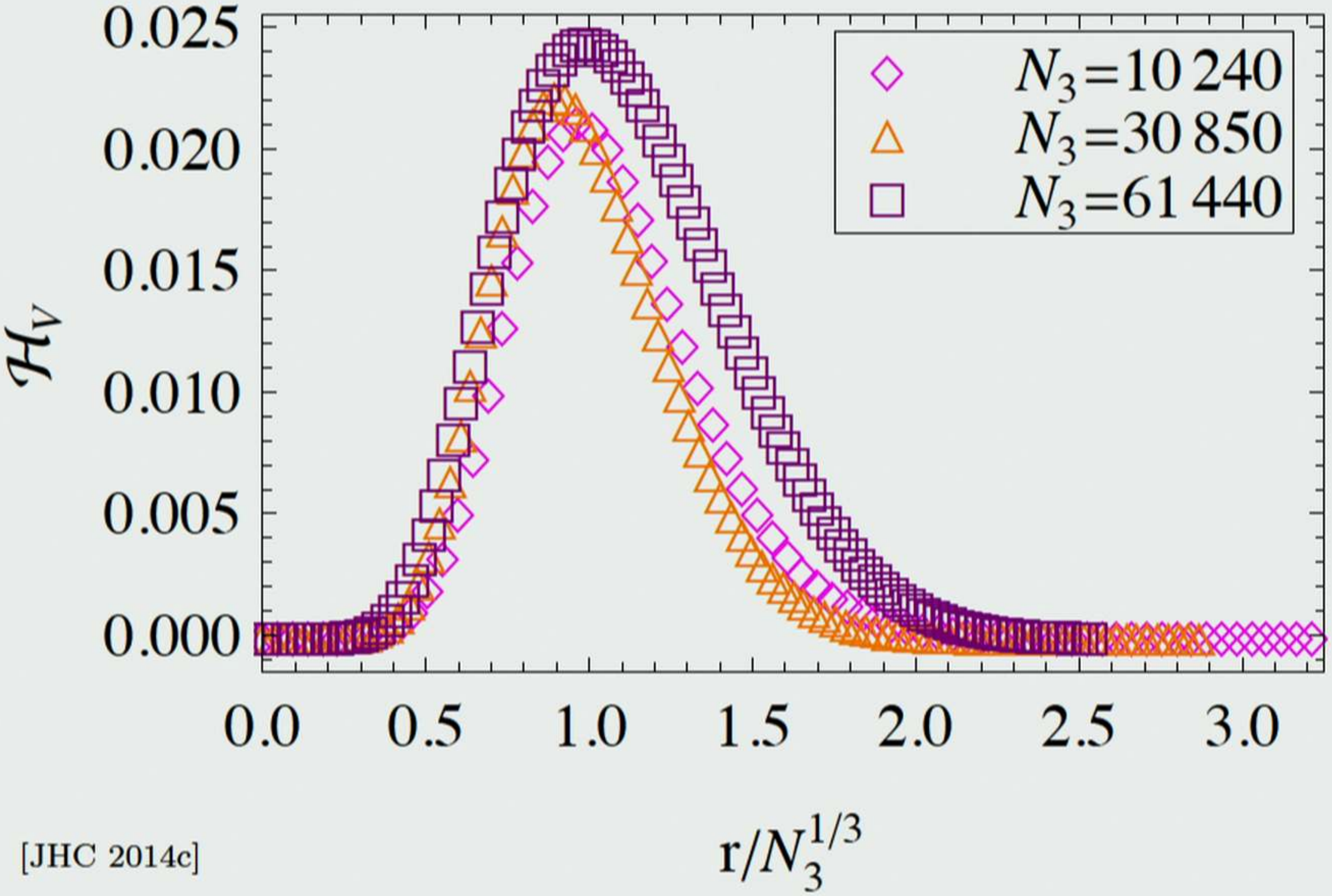

[JHC 2014c]

Temporal evolution of spatial volumetric homogeneity

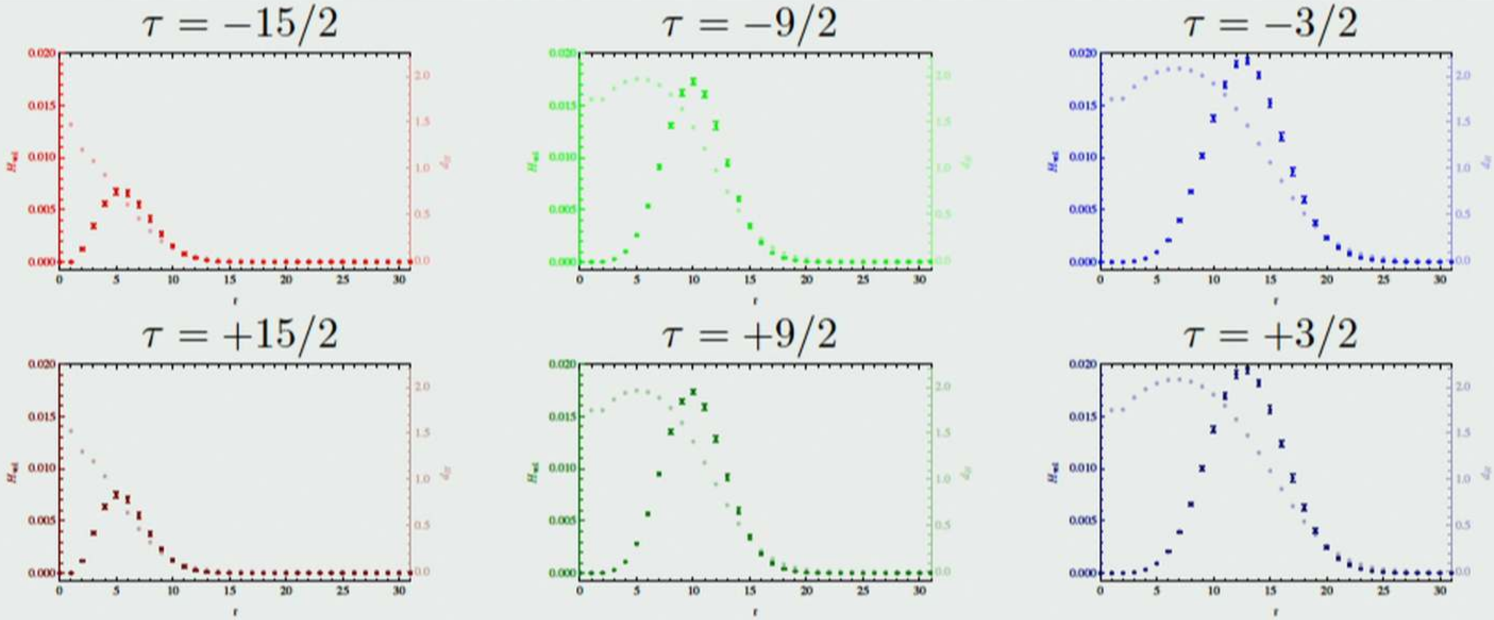

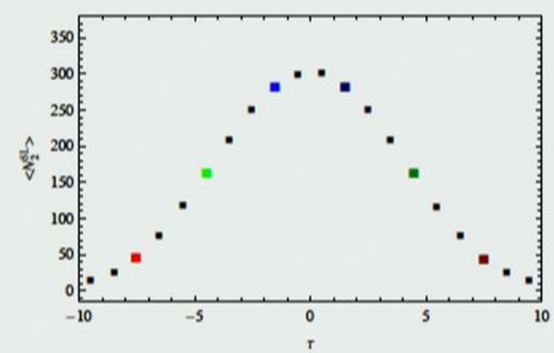

[JHC 2014c]

Scaling of inhomogeneity with discrete spatial volume

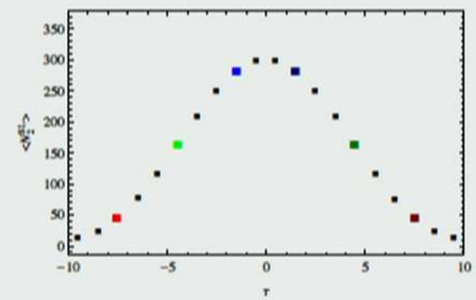

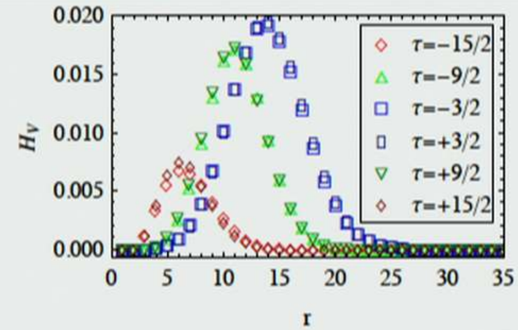

Typical scale $r_{\max}$ of inhomogeneity as a function of discrete spatial volume $\langle N_2 \rangle$

Increasing $\langle N_2 \rangle$

p=0.47 , R_{corr}=1.00

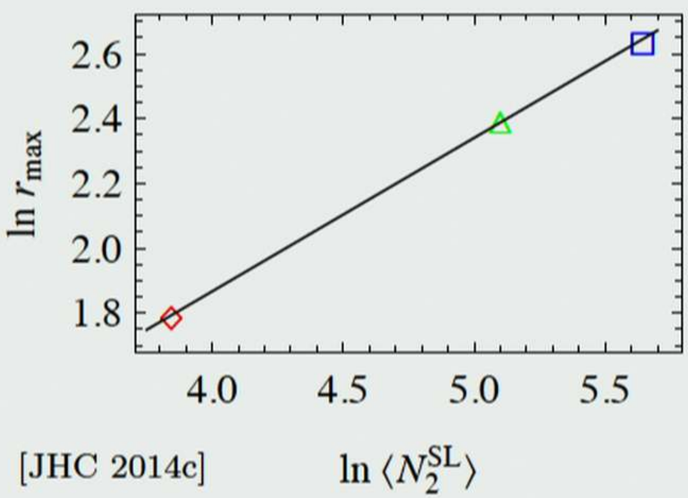

Decreasing $\langle N_2 \rangle$

p=0.46 , R_{corr}=1.00

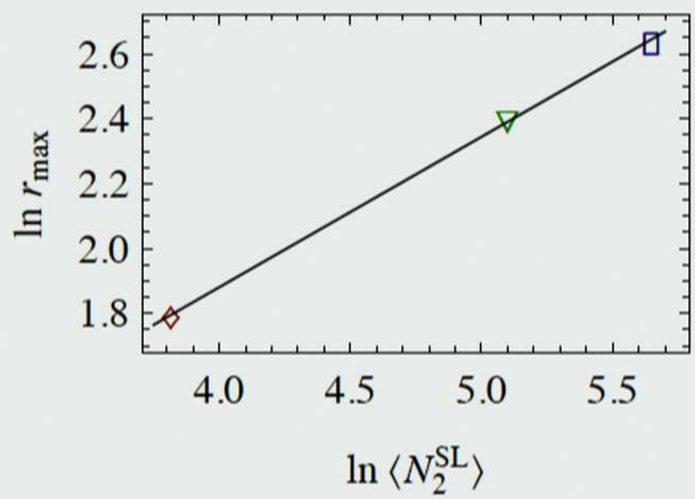

[JHC 2014c]

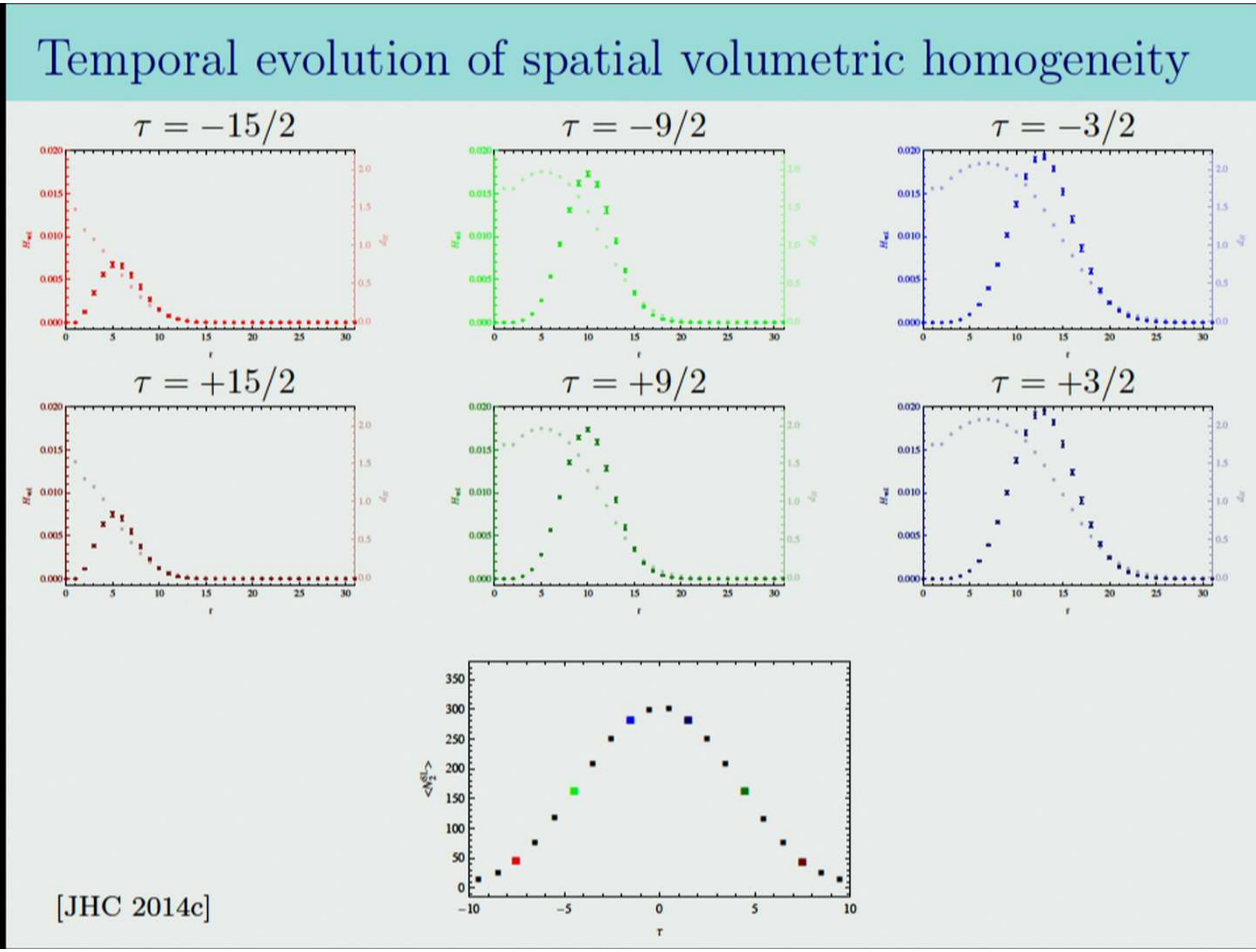
Temporal evolution of spatial volumetric homogeneity
τ = −15/2
τ = −9/2
τ = −3/2
τ = +15/2
τ = +9/2
τ = +3/2
[JHC 2014c]

Spectral homogeneity measure

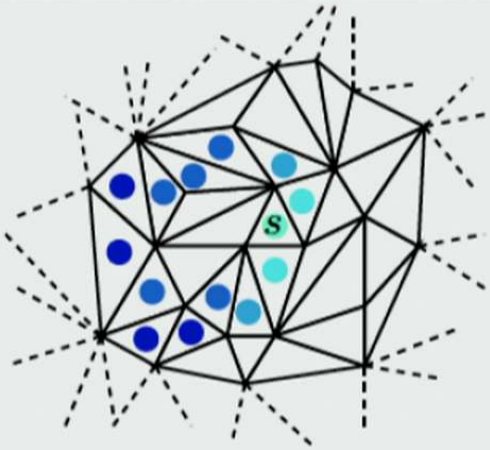

σ	$P_s(\sigma)$
0	1
1	1/4
2	1/4
3	5/32
4	17/128
⋮	⋮

[JHC 2014c]

- Return probability $P_s(\sigma) = K(s, s, \sigma)$
  - Mean

$$\mathrm{E}[P(\sigma)] = \frac{1}{N_D} \sum_{s \in \mathcal{T}} P_s(\sigma)$$

  - Variance

$$\mathrm{Var}[P(\sigma)] = \frac{1}{N_D - 1} \sum_{s \in \mathcal{T}} \{P_s(\sigma) - \mathrm{E}[P(\sigma)]\}^2$$

- Spectral dimension

$$D_s(\sigma) = -2 \frac{\mathrm{d} \ln \mathrm{E}[P(\sigma)]}{\mathrm{d} \ln \sigma}$$

- Homogeneity measure

$$\begin{aligned} H_{\mathrm{spec}}(\sigma) &= \langle \mathrm{Var}[P(\sigma)] \rangle \\ &= \frac{1}{Z_\Sigma} \sum_{\mathcal{T}} \mu(\mathcal{T})\, e^{-\mathcal{S}^{(\mathrm{E})}[\mathcal{T}]}\, \mathrm{Var}[P_{\mathcal{T}}(\sigma)] \end{aligned}$$

Spacetime spectral homogeneity

Ensembles of causal triangulations in phase C ($\mathcal{T}_c \cong S^2 \times S^1$, $k_0 = 1$)

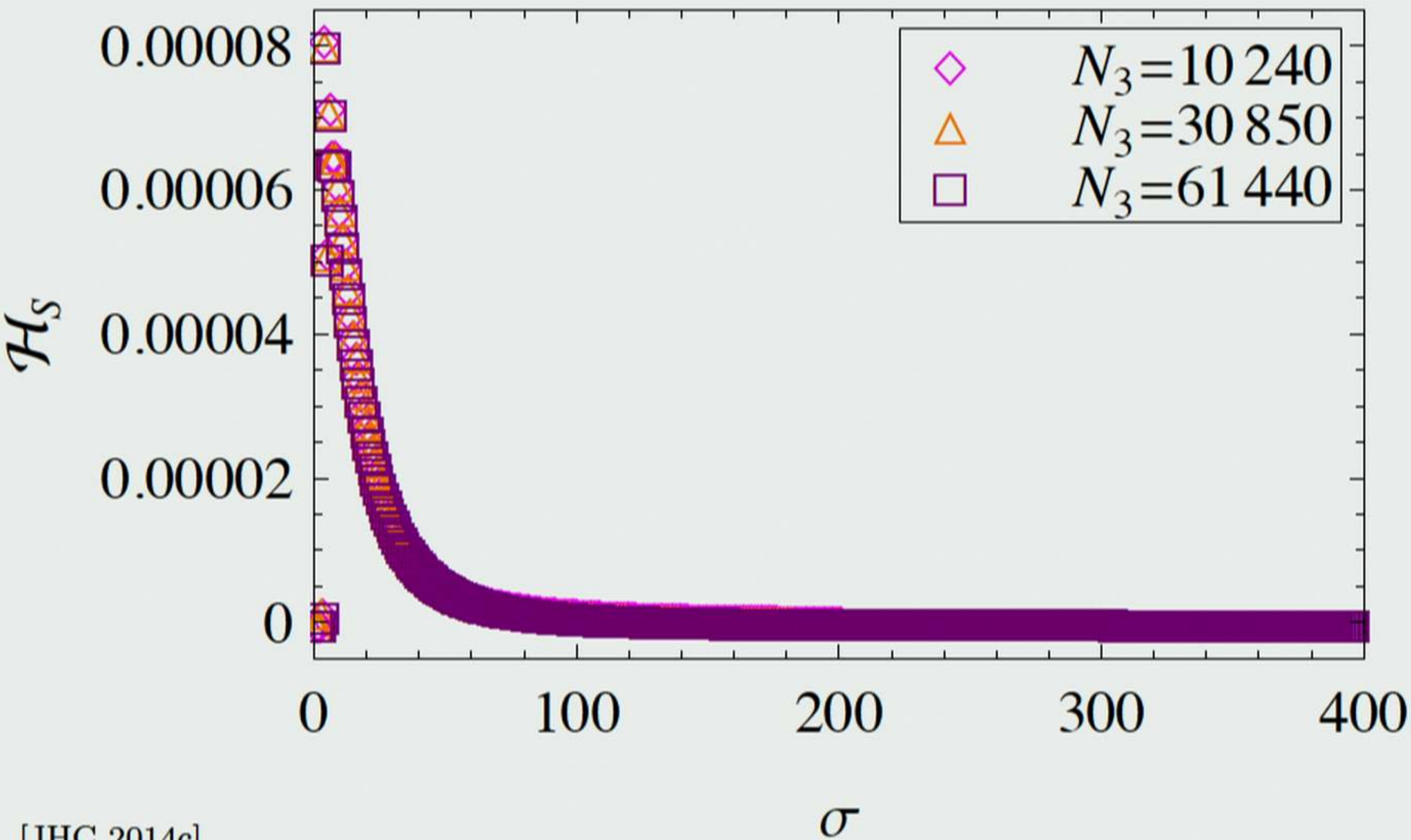

[JHC 2014c]

Third vignette: Effective actions in $2 + 1$ dimensions

A sample of transition amplitudes

Fixed initial and final leaves of the distinguished foliation ($\mathcal{T}_c \cong \mathrm{S}^2 \times [0,1]$)

Varying T, fixed N_3, fixed $N_2(\partial\mathcal{T}_c) = 4$

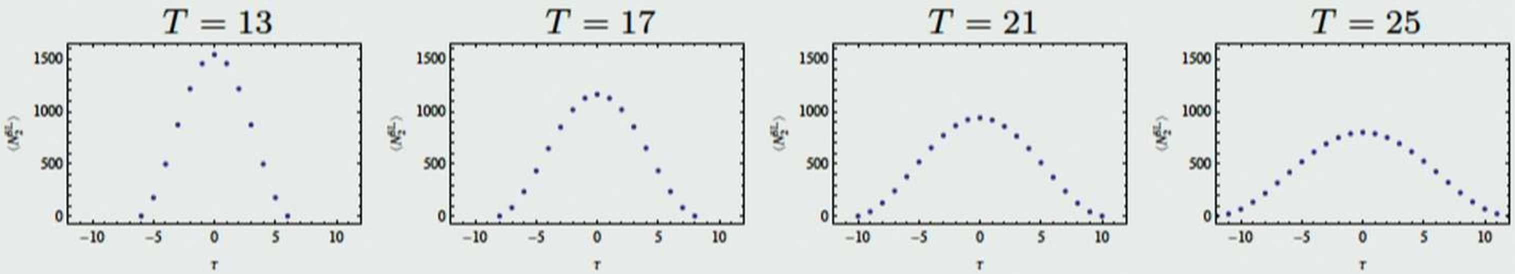

Varying $N_2(\partial\mathcal{T}_c)$, fixed N_3, fixed $T = 29$

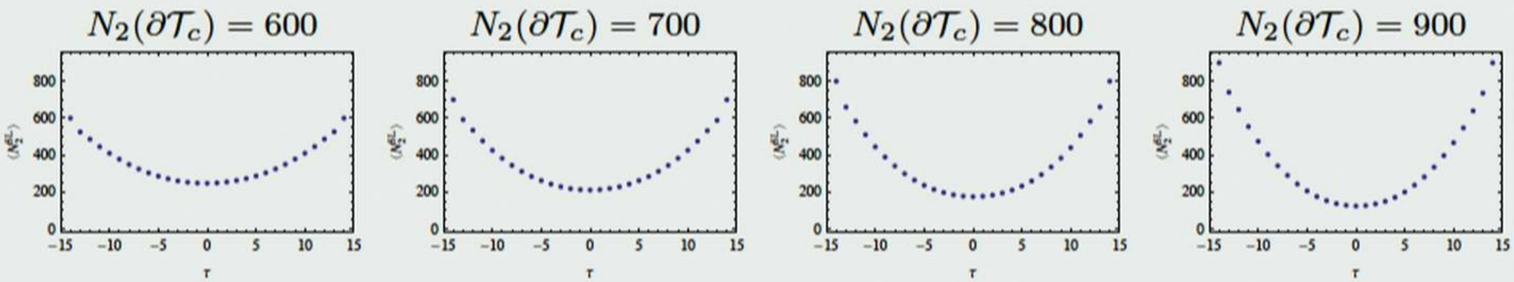

[JHC and Miller 2013], [JHC, Houthoff, Lee, and Miller 201?]

Second key result: classical limit

Large scale effective action for the discrete spatial volume $N_3(\tau)$

$$S_{\text{eff}}^{(\text{E})}[N_3] = c_1 \sum_\tau \left\{ \frac{[N_3(\tau+1) - N_3(\tau-1)]^2}{4N_3(\tau)} + c_2 N_3^{1/3}(\tau) + c_3 N_3(\tau) \right\}$$

Corresponding effective action for the continuous spatial volume $V_3(t)$

$$S_{\text{eff}}^{(\text{E})}[V_3] = \frac{1}{24\pi G_{\text{ren}}} \int \mathrm{d}t \sqrt{g_{tt}} \left\{ \frac{[\mathrm{d}V_3(t)/\mathrm{d}t]^2}{g_{tt} V_3(t)} + 9(2\pi^2)^{2/3} V_3^{1/3}(t) - \Lambda_{\text{ren}} V_3(t) \right\}$$

Extremum: Euclidean de Sitter space

$$V_3^{(\text{EdS})}(t) = 2\pi^2 \ell_{\text{dS}}^3 \cos^3\left(\frac{\sqrt{g_{tt}}\, t}{\ell_{\text{dS}}} \right)$$

Finite size scaled

$$\langle N_3^{(\text{EdS})}(\tau) \rangle \propto \frac{N_4}{s_0 N_4^{1/4}} \cos^3\left(\frac{\tau}{s_0 N_4^{1/4}} \right)$$

Ansatz $V_4 = \lim_{\substack{a\to 0 \\ N_4\to\infty}} C_4 N_4 a^4$

1-point function $\langle N_3(\tau) \rangle$

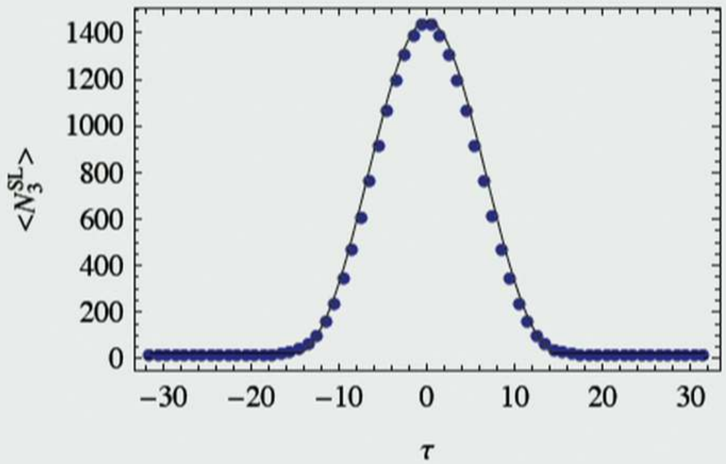

Determining the large scale effective action

- Benedetti and Henson provide evidence for the effective action of $(2+1)$-dimensional projectable Hořava-Lifshitz gravity
  - Explanation of the 'spacetime condensation' of phase C
  - Fits of deformed Euclidean de Sitter space to 1-point function $\langle N_2(\tau) \rangle$
  - Proposed scaling relations

[Benedetti and Henson 2014]

- Comprehensive statistical analysis
  - Consider several effective actions: Einstein gravity, projectable Hořava-Lifshitz gravity, fourth order gravity, *et cetera*
    - Perform fits to 1-point function $\langle N_2(\tau) \rangle$ and to connected 2-point function $\langle n_2(\tau) n_2(\tau') \rangle$
    - Perform statistical analysis to infer best explanation
  - Numerical tests of proposed scaling relations

[JHC, Houthoff, Lee, and Miller 2015]

Zeroth vignette: Euclidean dynamical triangulations

Reviving Euclidean dynamical triangulations

Renormalization group flows of quantum Einstein gravity (Einstein-Hilbert truncation)

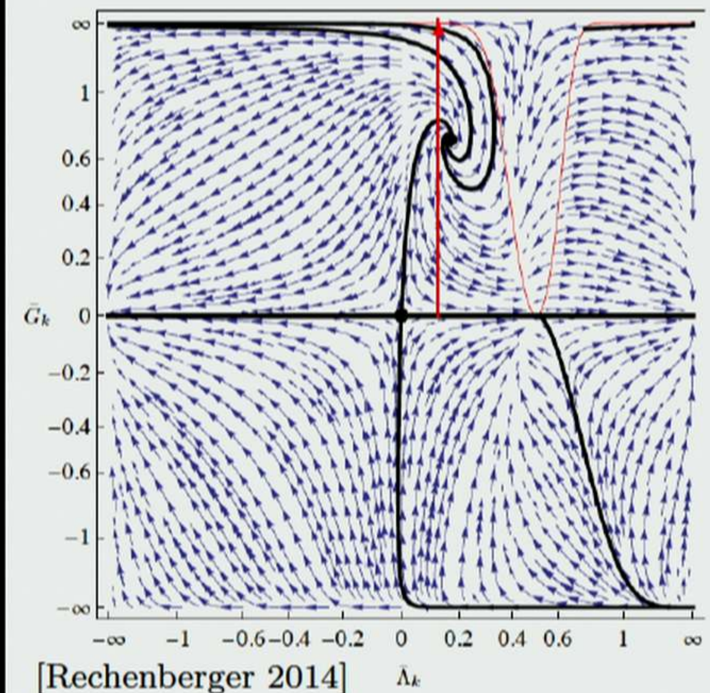

[Rechenberger 2014]

Corresponding phase diagram (Fixed $0 < \bar{\Lambda}_k < \bar{\Lambda}_k^c$, Varying $0 < \bar{G}_k < \infty$)

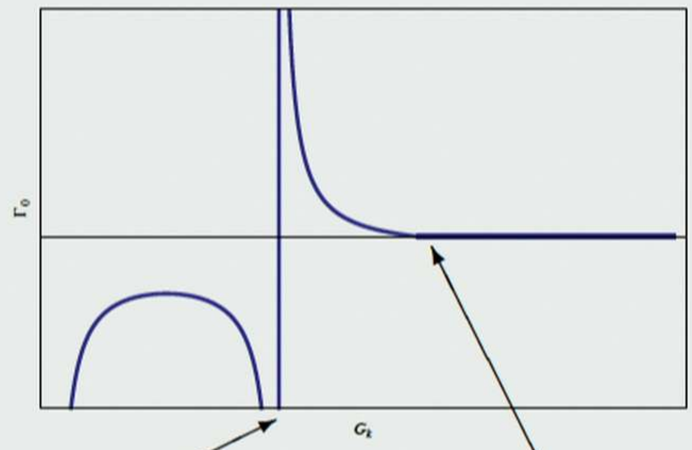

Partition function of Euclidean dynamical triangulation

$\mathcal{Z}_{\mathrm{EDT}} = \sum_{\mathcal{T}} \mu(\mathcal{T})\, e^{\kappa_2 N_2 - \kappa_4 N_4}$ for $\kappa_2 \sim G^{-1}$ and $\kappa_4 \sim G^{-1}\Lambda$

Search for a second order phase transition at $\kappa_2 \sim O(10)$

Key questions facing causal dynamical triangulations

1. Does causal dynamical triangulations admit a continuum limit in the form of an ultraviolet fixed point?
   - Not a necessary condition for viability (though probably a necessary condition for continued interest)
   - Further numerical studies near the BC phase transition, near the (hypothetical) ABC triple point, and at (hypothetical) end of AC phase transition
   - Further physical observables from numerical data for tracing renormalization group flows

2. Does causal dynamical triangulations admit a Newtonian gravity limit?
   - A necessary condition for viability
   - Attraction between quasi-point particles constructed as bundles of quasi-local energy (with K. Lee)

3. Can one formulate an Osterwalder-Schrader-type theorem for causal dynamical triangulations?
   - A necessary condition for interpretation of numerical results
   - Start from [Ashtekar, Marolf, Mourão, Thiemann 2000]